

STUDY OF THE STAIN FORMATION PHENOMENA IN PM PARTS

L. Aguirre and S. St-Laurent
Rio Tinto Metal Powders,
Sorel-Tracy, Quebec, J3R 4R4, Canada

Y. Thomas
National Research Council
Boucherville, Quebec, J4B 6Y4, Canada

ABSTRACT

Parts are produced by the PM process since many decades and stains appearing on the surface after the sintering process have been a recurring issue. Thus, comprehension of the phenomena and factors causing stain formation is essential for PM part producers. The current paper presents certain cases of stain formation and how to control the parameters to avoid it. When analyzing stains, MnS is found. Since the powder mix does not contain MnS, it is believed that its formation occurs during the delubrication process by a mechanism that needs to be further investigated. This paper presents the results of a study carried out to find probable causes of MnS formation on the surface of parts made from mixes containing no elemental MnS powder. In particular, samples tested in experimental conditions prone to stain formation were evaluated after delubrication and sintering stage to better understand the stain formation mechanism.

1. INTRODUCTION

Powder metallurgy (PM) technique is a manufacturing technology where metal powders, often mixed with a lubricant, are pressed into a specific shape followed by a sintering step. High volume precision components from steel powders can be produced with this method in an economic manner. Nevertheless, residual porosity in the finished part will result in lower mechanical properties compared to other methods such as machining from wrought materials, forging, precision casting and so forth. Therefore, the development of PM steels pre-alloyed or admixed with elements that produce higher strength parts was necessary. Common alloying elements include Mo, Ni and Cu. The prices of these alloying elements are highly variable in time [1] so the PM industry considered cheaper options such as Cr, Mn and Si [2]; however, these elements present high oxygen affinity and high vapor pressure, therefore pre-alloyed powders are preferred instead of the admix version [3]. Pre-alloyed water atomized powders with less than 0.2 wt% Mn are commonly used by the PM part manufacturers as they can achieve optimal heat-treated properties without sacrificing compressibility.

The final sintered density and strength of PM parts are not only driven by the powder formulation, but also by the compaction process and compacting conditions used, part geometry and furthermore the material behavior during sintering [4, 5]. Compaction techniques such as warm compaction and warm die compaction increase the ductility of the ferrous powder particles thereby increasing density [6,7,8,9,10]. The amount of lubricant has a strong effect on the maximum density that could be achieved during compaction, as lubricant has a very low specific gravity ($\sim 1 \text{ g/cm}^3$) compared to metallic powders. Indeed, the lower the lubricant content, the higher the maximum achievable density [5].

Lubricants are used in order to reduce particle to particle friction during pressing, facilitate ejection while reducing die-wall friction, produce parts with a good surface finish, delamination-free (due to springback), etc. Additionally, lubricants must be removed completely and cleanly during delubrication to avoid vapor accumulation that could burst and generate blisters but also to prevent sooting that could occur during sintering not only internally, preventing the bonding between the neighboring iron particles, but also externally as a surface stain.

Many studies have been carried out regarding the methods of lubrication, lubricant type and amount of lubricants [11,12,13,14,15,16,17], while other researchers focus on the delubrication properties of commonly used lubricants [18,19,20,21,22,23,24,25].

Staining of parts is a very complex phenomenon and depends on various parameters such as metal powder formulation, density of parts, delubrication and sintering conditions, furnace loading, heating rate, etc. It is the objective of this paper to investigate the nature of stains sometimes observed on some parts sintered in nitrogen/hydrogen atmosphere and try to understand the mechanism of stain formation. A case study of parts with a particular type of stain is presented.

Case of Study: Sintered Part with Small Stains Containing MnS

Staining has been an increasing issue for PM parts producers as industrial conditions demand higher production rates, implying an overload of the sintering furnaces and fast heating rates in the furnace profiles. While stains have been reported when using a variety of lubricants [17], their nature has always been referred to as “soot”.

Figure 1 shows an example of the presence of stains on sintered parts produced with a FC0208 mix. The green part is also shown to illustrate that the stain was not initially present on the part. The sintered part was analyzed with a SEM equipped with an energy dispersive x-ray (EDX) analyzer which revealed the presence of Mn and S mainly in the stain. The Mn/S peak ratio was very similar to that of MnS, which is very surprising since the powder mix contained no MnS in the form of elemental additive and the steel powder contains a low level of pre-alloyed Mn, 0.18%, and a very low level of sulfur, around 70 ppm. In fact, it is well known that for electrolytic Mn or FeMn containing mixes, Mn mass transfer occurs in the form of vapor [3, 26]. But in the case of a steel powder containing a low level of pre-alloyed Mn, the carrier mechanism causing the presence of MnS particulates at the surface of parts after sintering is still not understood.

It was thus decided to initiate a study with the objective of acquiring a better understanding of the stain formation mechanism for FC0208 materials sintered in a nitrogen-hydrogen atmosphere. The experimental conditions chosen were those mimicking the industrial conditions for which the stains rich in Mn and S were observed.

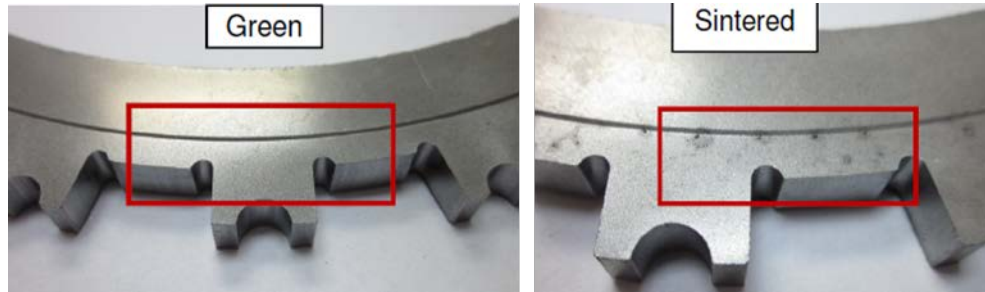


Figure 1. Sample of an industrial PM part presenting stains after sintering.

2. EXPERIMENTAL PROCEDURE

Stain-prone conditions were chosen to facilitate the analysis. The selected base powders used for this study were four water-atomized powders pre-alloyed with manganese at different concentrations and a granulated iron powder without Mn. Table 1 presents the nomenclature of the base powders used along with its Mn concentration, all powders contained less than 0.10 wt% O and 0.08 wt% S. Base powders were mixed with 1.5 wt% Cu, 0.6 wt% C and 0.75 wt% ethylene-bis-stearamide (EBS) wax.

Table 1: Type of base powders used and their Mn content.

Base Powder	Mn wt%	Type
BPA	0.20	Water atomized steel powder
BPB	0.13	
BPC	0.08	
BPD	0.04	
BPE	0	Granulated iron powder

Base powders and lubricant (EBS wax) were characterized with a thermogravimetric (TGA) analyzer, Metler Toledo TGA/DSC1 Star^c System, under a 100% N₂ (pre-purified grade 99.998%) atmosphere at a flow of 50 ml/min and heating conditions from 25°C to 550°C at a heating rate of 2, 20 and 40°C/min, for a sample weight of 6- 30 mg.

Uniaxial compacted TRS specimens with a height of 19.05 mm were pressed with a laboratory hydraulic press to a density of 7 g/cm³, following MPIF Standard 60 [27]. All samples were delubricated and sintered under a 90% N₂-10% H₂ atmosphere and same conditions:

- Delubrication: fast heating rate to reach 550°C dwelling of 25 min.
- Sintering: fast heating rate till 800°C followed by slower heating rate from 800-1130°C, with a dwelling time of 25 min at 1130°C.

These thermal conditions were tested, as they are known to be contributing factors for an improper delubrication and promote surface oxide enrichment [3, 23,28].

Steel powder, delubricated and sintered bars were analyzed with a JEOL JSM-6490 scanning electron microscope (SEM) coupled with an energy dispersive x-ray (EDX) spectrometer OXFORD X-MAX 80mm, with an INCA platform. Secondary electron imaging (SEI) and backscattered electron imaging (BEI) modes were used to better visualize the topography and composition of the base powder, bars and stains.

3. RESULTS AND DISCUSSION

3.1 Mix characterization: Base powders and lubricant

Water atomized steel powder pre-alloyed with Mn was analyzed using SEM and EDX, a picture of BPA taken in the SEI mode is shown in Figure 2 with indications where EDX analyses were performed and analyses results are reported in Table 2. It is important to mention that the oxygen percentage is obtained by a stoichiometric calculation from the data obtained with the EDX analyzer and the minimum limit of detection of the later is 0.1%. Some oxide particles could be observed on the powder surface in the spectra that were taken, likely complex Si-Mn-Cr oxides, but no MnS particles were found. Very little sulphur was detected, confirming that the sulphur content is kept below 70 ppm for this type of steel powders.

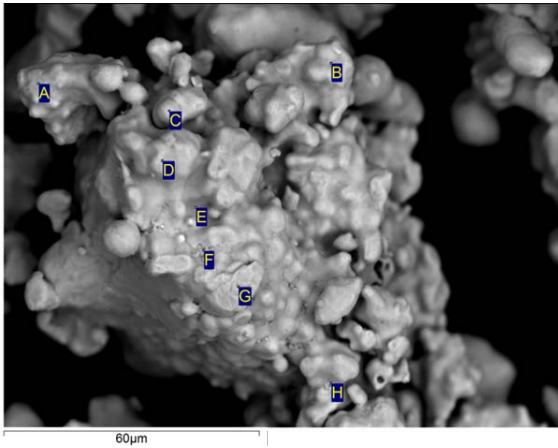


Figure 2. SEI micrograph of BPA water atomized steel powder. Letters indicate where EDX spot analyses were performed.

Table 2: EDX analysis at specific locations of the water atomized steel powder.

Spectrum	O	Si	S	Cr	Mn	Fe
A	1.27	0.00	0.00	0.10	0.14	98.49
B	1.16	0.12	0.00	0.00	0.23	98.49
C	0.39	0.06	0.00	0.15	0.35	99.05
D	0.29	0.06	0.00	0.00	0.23	99.42
E	0.23	0.00	0.00	0.11	0.61	99.05
F	0.12	0.06	0.13	0.00	0.19	99.50
G	0.80	0.10	0.00	0.09	0.28	98.73
H	1.04	0.16	0.00	0.12	0.42	98.26

All elements in wt%

Most popular lubricants used in PM consist mainly of two different types of fatty acid based wax compounds: organic waxes such as EBS and metallic stearates such as zinc stearate (ZnSt). Organic waxes typically decompose cleaner than the metallic stearates. As seen on the TG graph of Figure 3, the organic waxes decomposed completely while ZnSt and Kenolube would have a weight-loss of 84.2% and 90.2%, respectively. As metallic stearates will leave residues, EBS wax was selected for this study to avoid interactions of the metallic ions from the lubricant and interference in the stain chemical analysis.

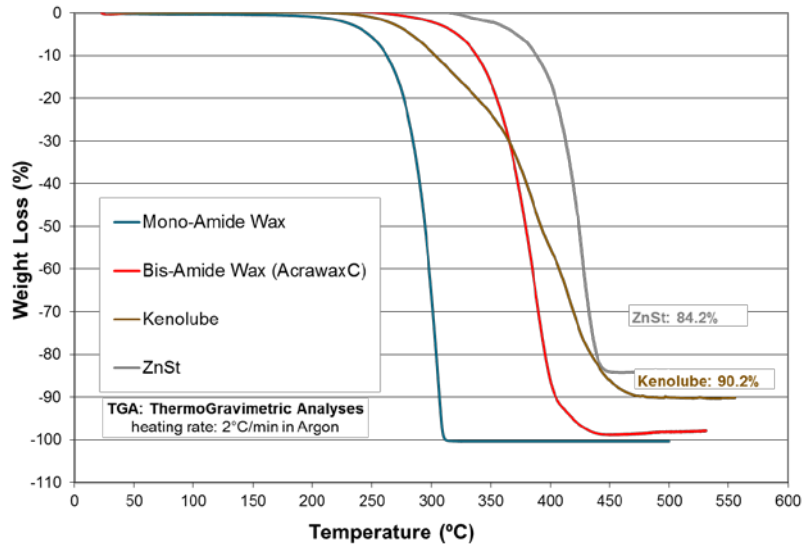


Figure 3. TG analysis of various organic waxes and lubricants composed partially or fully of metallic stearates, ran at a heating rate of 2°C/min under 100% Ar atmosphere at a flow of 50 ml/min.

A number of complex chemical and physical processes can be expected to occur, often simultaneously, between the onset of lubricant thermolysis and sintering. These include: 1) Decomposition of organic species (EBS will break down into smaller hydrocarbons, CO₂, CO and NH₃) [18]; 2) Chemical interactions between these species and the surfaces of the compacted metal powders; in the base powder as temperature increases there will be a mass transfer of elements with high oxygen affinity to the powder surface, with the formation of stable oxides, but with low carbothermal reduction conditions these oxides can transform to more complex oxides [28]; 3) Mass transport of reactants, volatile species, and degradation products through porosity channels; 4) Changes in the distribution of liquid-phase lubricant within the pore structure of the compact, etc. [20].

TG analysis was performed on EBS wax at different heating rates and as shown in Figure 4, the heating rate plays an important role in the pyrolysis of EBS wax. At faster heating rates, EBS wax decomposition will complete at a higher temperature and vice versa. For instance, at a heating rate of 2°C/min, full decomposition was achieved at 400°C while at heating rate of 40°C/min, decomposition was concluded at a temperature 75°C higher.

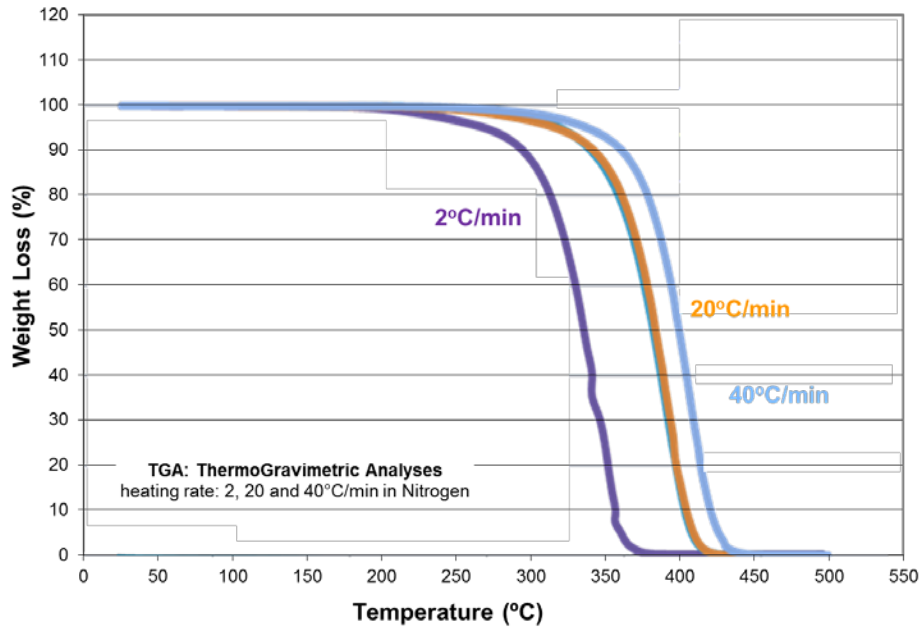


Figure 4. TG analysis of EBS wax ran at heating rates of 2, 20 and 40°C/min under 100% N₂ atmosphere with a flow of 50 ml/min.

When performing a TG analysis on the powder mix (base powder + 0.6 wt% C + 1.5 wt% Cu + 0.75 wt% EBS wax) at 20°C/min (Figure 5) an acceleration of the decomposition of the EBS wax is observed at a temperature of 400°C, which is about 50°C less than for the lubricant on its own. This is related to the presence of metal powder such as Cu and the base powder itself, which behave as catalysts since hydrolysis occurs via a metal-mediated process [20]. After full lubricant decomposition the powder starts to gain weight as some oxidation on the powder surface is taking place.

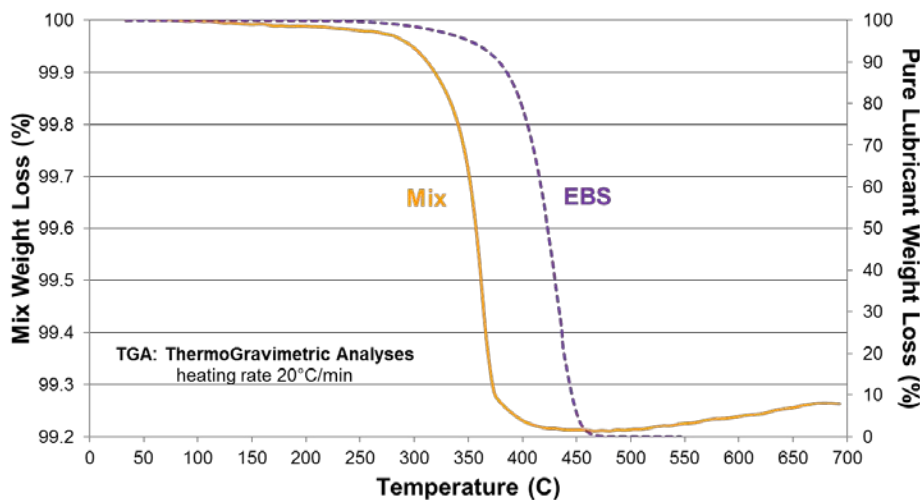


Figure 5. TGA results for the powder mix (base powder + 0.6 wt% C + 1.5 wt% Cu + 0.75 wt% EBS wax) and EBS wax ran at a heating rate of 20°C/min under N₂ atmosphere.

3.2 Sintered part characterization

3.2.1 Effect of the base powder

The different base powders (Table 1) were mixed with 1.5 wt% Cu, 0.6 wt% C and 0.75 wt% EBS wax. The mixes were pressed to a density of 7.0 g/cm³ and sintered under a 90% N₂-10% H₂ atmosphere. Table 3 shows the degree of staining on a part surface after sintering as a function of the Mn content on the pre-alloyed powder.

There is a clear correlation between the amount of Mn content in the base powder and the degree of staining. To higher Mn content in the steel powder, more stains are observed on the part surface. Moreover, for an iron powder containing no Mn, the surface of the bar is clean. It is important to note that the stain formation is mostly at the bottom of the part suggesting that there is the effect of gravity on the viscous or liquid lubricant as it exits the part during its decomposition

Table 3: Lateral view of sintered TRS bars produced from the same mix formulation (BP + 1.5 wt% Cu + 0.6 wt% C + 0.75 wt% EBS wax) containing a base iron powder of varying Mn content.

Base Powder	Sintered bar
BPA 0.18 wt% Mn	 <div style="display: flex; align-items: center; justify-content: center;"> <div style="margin-right: 5px;">Top</div> <div style="margin-right: 5px;">↑</div> <div style="margin-right: 5px;">↓</div> <div style="margin-right: 5px;">Bottom</div> </div>
BPB 0.13 wt% Mn	
BPC 0.08 wt% Mn	
BPD 0.04 wt% Mn	
BPE 0 wt% Mn	

3.2.2 Stain composition after sintering

To know the nature of the stain after sintering, EDX analysis was performed on what seems to be particulates which precipitated on the part surface. A picture of such a stain is shown in Figure 6 where spot or map analyses are indicated by letters or a square respectively. The results of EDX analyses reported in Table 4. Particular attention is given to the area of analysis D, which evidently shows that the stain is rich on Mn and S, but the presence of other elements such as Ca and Mg are not to be neglected since they suggest the oxidation of alloying elements (possibly formation of complex oxide spinels) that were transported to the part surface by a mechanism that requires further investigation. The nature of the stains observed during our tests was identical to that observed on parts produced under real production conditions, clearly demonstrating that our laboratory conditions reproduced the conditions that existed during the production of the parts.

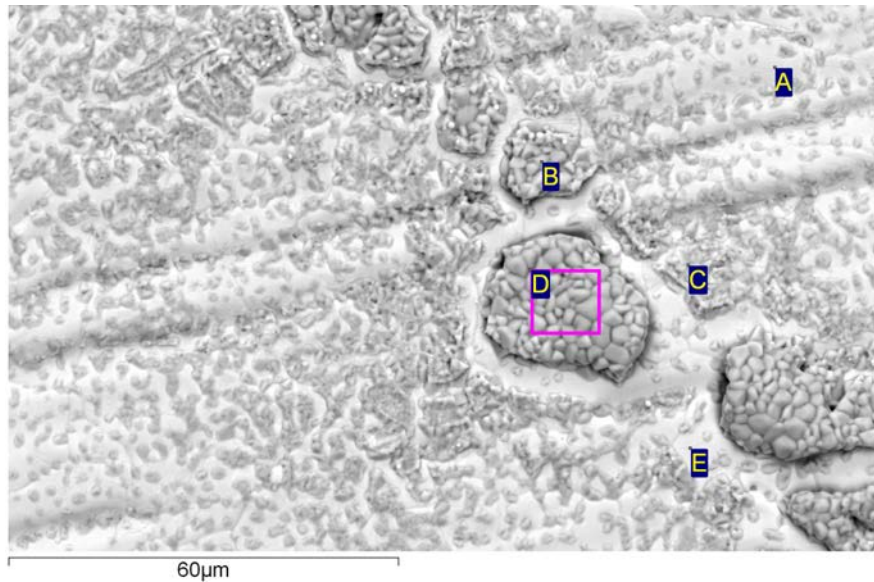


Figure 6. SEI micrograph of a stain on the surface of a TRS bar after sintering. Letters indicate where EDX spot or area of analysis was performed.

Table 4: EDX analysis at specific locations of the water atomized steel powder.

Spectrum	C	O	Mg	Si	S	Ca	Cr	Mn	Fe	Cu
A	2.30	0.90	0.00	0.00	0.11	0.00	0.00	0.42	87.09	9.19
B	4.64	1.68	2.22	0.11	35.95	7.54	0.00	44.10	2.82	0.94
C	6.27	1.01	1.73	0.09	18.51	3.75	0.12	23.17	43.82	1.52
D	4.93	2.08	2.40	0.17	36.15	7.43	0.00	43.57	2.42	0.85
E	2.62	0.68	0.00	0.09	0.29	0.10	0.00	0.59	93.94	1.69

All elements in wt%

3.2.3 Effect of copper on the stain formation

It was noted that copper was often found in the area of deposition (as listed in Table 4); therefore a similar mix using BPA and no copper was prepared, pressed and sintered under the same conditions.

Surprisingly, very little or no stains were found on the sample without copper, as illustrated in Table 5.

The role of copper in the stain formation could be: 1) as a more efficient catalyst, since its particle size is smaller than the steel powder, promoting faster lubricant thermolysis and/or 2) accelerating the reaction interphase between lubricant and steel powder. For the purpose of this work it was included in the mix as it is a key factor in the stain formation containing MnS particulates.

Table 5. Lateral view of sintered TRS bars produced from a BPA-based mix with or without Cu.

BPA + wt% Cu + 0.6 wt% C + 0.75 wt% EBS wax		
	0 wt% Cu	1.5 wt% Cu
0.18 wt% Mn		

3.3 Delubricated part characterization

In order to understand how MnS is found on the surface of the part, heat treatment of the TRS bars was interrupted after the delubrication step at 550°C during 25 min. This temperature was chosen as we go beyond the decompositions temperature of EBS wax and with a fast heating rate to shift the EBS wax decomposition to a higher temperature, as seen on Figure 4.

The delubricated bars were analyzed with SEM, where an EDX mapping presents in brighter areas higher concentrations of selected elements. A map analysis done on the deposits after delubrication (Figure 7) showed the presence of carbon, oxygen and manganese, but no sulphur. A similar analysis was done on sintered bars (Figure 8) and clearly the amount of carbon and oxygen on the stain decreased, likely after reducing in gaseous CO and CO₂ species, which are carried away from the part by the flowing atmosphere of 90% N₂-10% H₂. The hydrogen atmosphere can possibly react with the base powder to produce sulfuric acid with in turn could leach Mn from the powder surface. The Mn at this point will react with sulphur to form MnS.

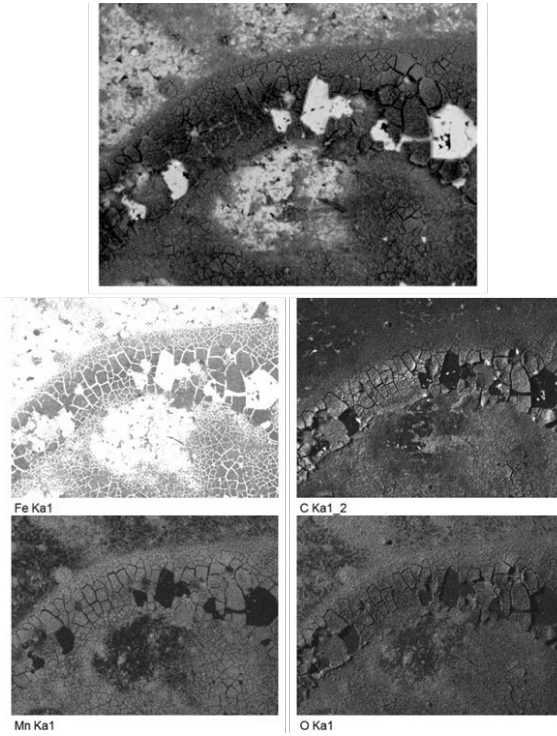


Figure 7. SEI micrograph of a stain on the surface of a TRS bar after delubrication and EDX map analysis of Fe, C, Mn and O.

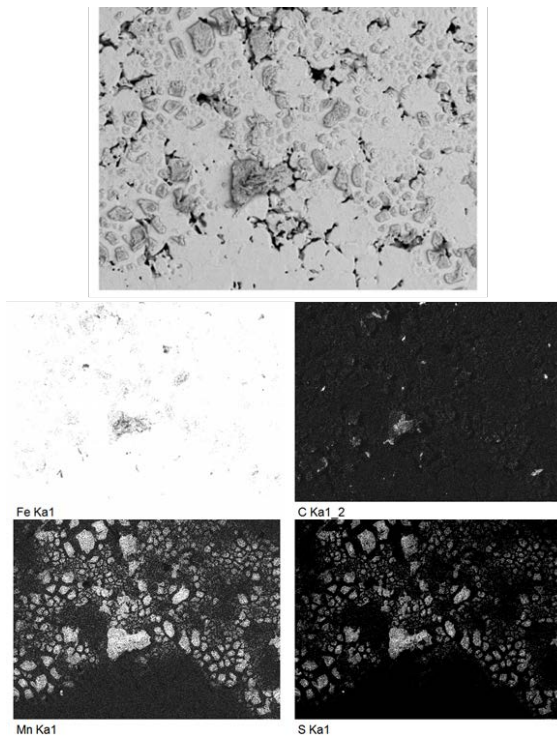


Figure 8. SEI micrograph of a stain on the surface of a TRS bar after sintering and EDX map analysis of Fe, C, Mn and S.

3.3.1 Origin of the delubrication deposit

After delubrication (550°C) a deposit rich in Mn-O-C is found on the part surface, nevertheless, the origin or depth from which manganese comes (from the surface of the part or carried from inside the part) is not known. To understand this mass transfer mechanism, co-filling of the die with the aid of a splitter was performed in order to press TRS bars with two layers of mix powder (BPA and BPE) vertical to the compaction pressure. This was done in order to constantly evaluate the same faces of the TRS bars through the entire study. Figure 9 shows a schematic representation of a TRS bar with the distribution of the 2 layers thickness, and the delubricated bars with BPA and BPE. It is important to note that only the base powder changed on the mix composition.

Delubrication of the bars showed that when BPE (iron powder) is thicker (10 mm) most of its surface is clean, but when the thinner layer is BPE deposits can form on the surface. This proves that Mn-rich deposits originate from inside the part (at least 2 mm depth) and are carried to the surface in a mass transfer mechanism which needs to be further studied. As it has been reported [23], extended dwell time of the pre-alloyed powders at higher temperatures than ~500°C is not recommended, since increased temperature leads to improved mass-transfer of alloying elements on the powder surface and their further oxidation. The enrichment of the powder surface in stable oxides is connected with the second stage of lubricant decomposition when high amount of CO₂ is produced but still does not explain the transfer of Mn rich components to the surface of the part.

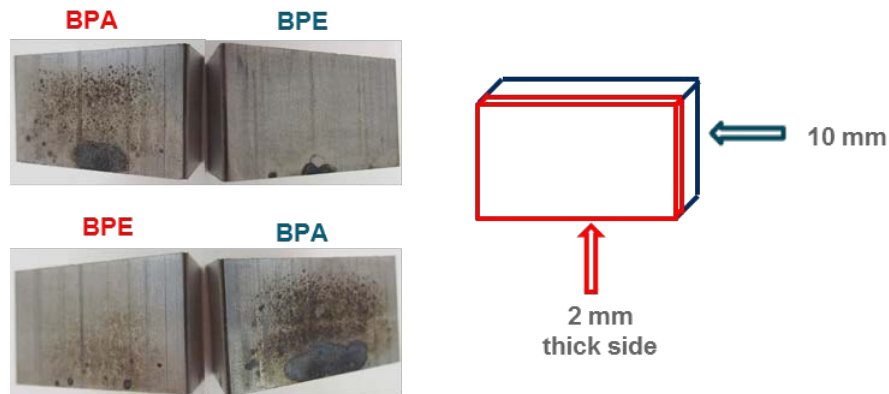


Figure 9. Delubrication of TRS bars composed of a double layer of base powders (BPA and BPE) pressed vertically.

3.4 Plausible MnS formation mechanism

A schematic diagram illustrating the decomposition process of a lubricant in a compacted mix composed of steel powder, graphite and admixed copper is represented in Figure 10 and proposes a potential mechanism for the formation of MnS stains at the surface of parts during sintering. At the first stage, as temperature is raising the lubricant is brought to its melting point, swells and starts to fill open porosities and channels to reach the surface of the part. Then, at a temperature of 250-500°C, lubricant thermolysis takes place, breaking down into smaller hydrocarbons, CO₂, CO and NH₃ [18]. These vapors start pressurizing other residues towards the surface.

At the same time, the presence of copper increases the chemical potential of carbon onto the steel network [29], helping admixed graphite and carbon oxides (from the lubricant byproducts) react with the steel powder. From this point (400-750°C), the interaction of lubricant byproducts with the powder surface

leads to oxidation of pre-alloyed powders while carbothermal reduction of surface oxides takes place [22]. By analyzing the delubricated parts (heat treatment at 550°C), and finding stains rich in Mn-O-C, it is suggested that the reaction of carbon oxides with the surface of the steel powder produces complex manganese containing products. These complex Mn-O-C products are pushed to the surface by the continuous pressure generated from the lubricant decomposition.

Afterwards, the steel powder continues to reduce, manganese oxides can be reduced and free manganese can react with segregated sulphur forming MnS and will remain at the surface of the part. In fact, when heating MnO with CO at 780°C a reversible reaction of Mn with CO₂ is produced [30]. It is believed that when this equilibrium is attained the MnS will form. Reduction of MnO at higher temperature when a very low dew point atmosphere is used is also possible, especially with the presence of carbon (from the graphite) that helps increasing the reducing potential conditions at high temperature (to be demonstrated by thermodynamics). Additionally, sulphur from the base powder surface can react with the H₂ atmosphere to possibly form sulfuric acid that can further reduce MnO to form MnS and H₂O.

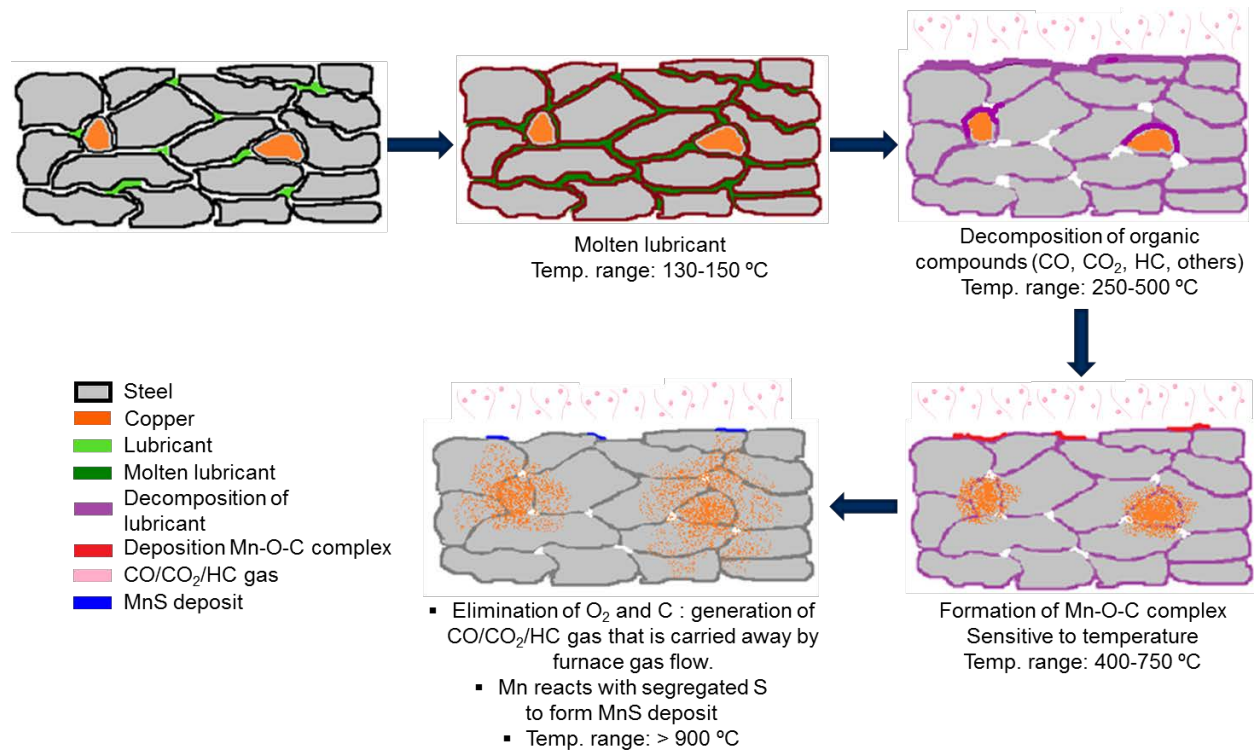


Figure 10. Schematic diagram of the decomposition process of the lubricant, interaction with the metallic powders and process of stain formation containing MnS on the sintered part.

4. CONCLUSIONS

It is common in PM to observe the presence of stains at the surface of parts after sintering when particular conditions are met (large part, large amount of lubricant and/or graphite, fast heating rate during delubrication, or improper sintering profile, very dry and pure sintering atmosphere, etc.). The results of a study carried out to better understand the formation mechanism of MnS stains found at the surface of parts containing no elemental MnS and very low levels of Mn and sulfur were presented.

The stain formation mechanism of stains containing MnS can happen in a two-step simultaneous process:

1. Mn from the steel powder reacts with lubricant decomposition by-products (CO, CO₂, HC) inside the part. This co-product is expelled out of the part due to internal gas pressure and deposits at the surface of the part. Therefore, after delubrication, Mn, O and C were uniformly distributed in the deposit. Later, the carbon and oxygen in the deposit are eliminated in the hot zone of the furnace, sulfuric acid can be formed from the sulphur in the base powder and the sintering atmosphere which leaches Mn from the base powder to form MnS.
2. As temperature increases (780°C), MnO from the surface of the steel powder can be reduced to Mn, evaporating and migrating to the surface of part where it reacts with segregated sulphur producing MnS.

The exact mechanism for the Mn-C-O complex formation is not fully understood. But our tests confirmed that Mn can travel with this complex product from the inner portion of the part and deposit at the surface where further reduction of carbon and oxygen take place and where remaining manganese reacts with sulphur, leaving a precipitate mainly composed of MnS.

It is the objective to pursue our investigation and find conditions or solutions to eliminate or limit the formation of MnS stains such as described in this paper. For instance, it is interesting to mention that additional tests were performed modifying the delubrication conditions and resulted in stain-free parts. These delubrication conditions were: slow heating rate and dwelling at 400°C to accomplish proper delubrication before reaching sintering temperature.

ACKNOWLEDGEMENTS

The authors wish to express their gratitude to the following people for their dedicated involvement in the present study: Dany Richard, Claude Gelinias and Olivier Bouchard (RTMP) for the preparation and testing of mixes in the quality control laboratory, Donald Brunelle and Vincent Richard (RTIT) for the SEM characterization, and Dominique Desgagnés (NRC-Canada) for TGA experiments.

REFERENCES

-
- ¹ Frykholm, R. and S. Bengtsson, "New alloy designed for heat treated applications", *Proceedings of the 2010 Powder Metallurgy*, World Congress, 2010, pp. 1-8.
 - ² Hryha, E. and E. Dudrova, "The Sintering Behaviour of Fe-Mn-C Powder System, Correlation between Thermodynamics and Sintering Process, Manganese Distribution and Microstructure Composition, Effect of Alloying Mode", *Application of Thermodynamics to Biological and Materials Science*, P.M. Tadashi, Editor. 2011, In. Tech.
 - ³ Hryha, E., et al., "Sintered Steels Alloyed with Manganese: Effect of Alloying Mode", *PM2010 World Congress*, (Sintered Steels: Mechanical Properties) 2010, pp. 1-8.
 - ⁴ St-Laurent, S., F. Chagnon, and Y. Thomas, "Study of Compaction and Ejection Properties of Powder Mixes Processed by Warm Compaction", *Advances in Powder Metallurgy and Particulate Materials*, 2000, pp. 3.79-3.91.
 - ⁵ Aguirre, L., S. St-Laurent, and Y. Thomas, "Comparison of Various Lubricant Systems and Compaction Methods for High Density Applications", *Proceedings of the 2013 International Conference on Powder Metallurgy and Particulate Materials*, 2013, pp. 3.60-3.72.

-
- ⁶ Bocchini, G.F., “Warm Compaction of metal powders. Why it works, why it requires a sophisticated engineering approach”, *Advances in Powder Metallurgy & Particulate Material*, 1998, vol.1, pp. 4.29-4.42.
- ⁷ Chagnon, F., C. Gélinas, and Y. Trudel, “Development of High Density Materials for P/M Applications”, *Advances in Powder Metallurgy & Particulate Material*, 1994, Vol.3, pp. 199-206.
- ⁸ Gagné, M., “Warm and Cold Compaction”, *Advances in Powder Metallurgy and Particulate Materials*, 1997, vol.1, pp. 319-206.
- ⁹ Musella, V. and M. D'angelo, “Process for Preheating Metal in Preparation for Compacting Operations”, U.S. Patent No. 4,955,798/1990: United States.
- ¹⁰ Chagnon, F. and Y. Trudel, “Effect of Compaction Temperature on Sintered Properties of High Density P/M Parts”, *Advances in Powder Metallurgy and Particulate Materials*, 1995, vol. 2, pp. 5-3.
- ¹¹ Hammond, D.L., “Lubricant system for use in powdered metals”, US Patent 6,679,935, issued on January 20, 2004.
- ¹² Hanejko, F.G., “Methods for preparing metallurgical powder compositions and compacted articles made from the same”, US Patent Application 20070186722, 2006.
- ¹³ St-Laurent, S., Y. Thomas, and L. Azzi, “High Performance Lubricants for Demanding PM Applications”, *Proceedings of the International Conference On Powder Metallurgy and Particulate Materials*, 2006.
- ¹⁴ Azzi, L., Y. Thomas, and S. St-Laurent, “Lubricants for high-density compaction at moderate temperatures”, *International Journal of Powder Metallurgy*, 2007, vol. 43, no. 6, pp. 39-46.
- ¹⁵ Ahlin, A., A. Ahlqvist, and O. Litström, “Newly developed lubricants for high performance metal powder mixes”, *Proceedings of the International Powder Metallurgy Congress & Exhibition*, 2008, vol. 3 (Euro PM2008).
- ¹⁶ Wimbirt, L., et al., “Advanced Lubricants - A Complex Challenge for Powder Metallurgy: Density, Lubricity, Environment”, *Proceedings of the World PM2010 Congress & Exhibition*, EPMA, 2010. vol. 1.
- ¹⁷ McQuaig, K., Schade, C., Sokolowski, P., “Development of a Lubricant System for Improved Performance of Premixes”, *International Conference on Powder Metallurgy and Particulate Materials*, 2013, pp. 3.60-3.72.
- ¹⁸ Bolarin, A. M. and Sanchez, F., “Elimination of the lubricant in metal powder compacts”, *EuroPM2003*, 2003, pp. 291-300
- ¹⁹ Gateaud, A., “Physical and Chemical Mechanisms of Lubricant Removal During Stage I of the Sintering Process”, 2006, Master Thesis, Worcester Polytechnic Institute.
- ²⁰ Baum, M.M., Becker, R.M., Lappas, A.M., Moss, J.A., Apelian, D., Saha, D., and Kapinus, V.A., “Lubricant Pyrolysis during Sintering of Powder Metallurgy Compacts”, *Metalurgical and Materials Transactions B*, vol 35B, 2004, pp.381-392.
- ²¹ Kawano T., Ono T., Ozaki, Y., “Analysis of Dewaxing Behavior of Iron Powder Compacts Based on a Direct Observation of Decomposing Lubricant During Sintering in a Furnace”, *JFE Technical Report No. 16*, 2011, pp. 83-88.
- ²² Hryha, E., S. Karamchedu, and L. Nyborg, “Delubrication of PM Components Based on Cr-Prealloyed Steel Powder - Chances and Risks”, *Proceedings of the 2011 Euro PM 2011*, vol.3 (Sintering - Atmospheres & Atmosphere Controls), pp. 105-110.
- ²³ Hryha, E., S. Karamchedu, and L. Nyborg, “Control of delubrication process for PM components based on prealloyed steel powders”. *Proceedings of the 2012 Powder Metallurgy World Congress & Exhibition*, 2012, (16C-T2-10).
- ²⁴ Hryha, E.; Nyborg, L., “Process Control System for Delubrication of PM Steels”, *Acta Metallurgica Slovaca* 2012, vol. 18, no. 2-3, pp. 60-68.
- ²⁵ Malhotra, R. P., “Effective Lubricant Removal for Sintering of Iron Parts”, *Proceedings of the 2013 International Conference on Powder Metallurgy and Particulate Materials*, 2013, pp. 3.60-3.72.

-
- ²⁶ Salak, A. and Selecka, M., “Adverse Effect of High Purity Atmosphere on Sintering of Manganese Steels”, *Powder Metallurgy*, 2010, vol. 53, pp. 285-295.
- ²⁷ *MPIF Standard Test Methods for Metal Powders and Powder Metallurgy Products*. 2012, Metal Powder Industries Federation: Princeton, NJ (USA).
- ²⁸ Hryha, E. and L. Nyborg, “Oxide Transformation During Sintering of Cr and Mn Prealloyed Water Atomized Steel Powder”, *Proceedings of the Euro PM2011*, 2011, vol.1 (Sintered Steels), pp. 95-100.
- ²⁹ Nabeel, M., “Diffusion of Elemental Additives during Sintering”, 2004, Master Thesis, Royal Institute of Technology, Sweden.
- ³⁰ Campbell, A.N. and Brown, E. A., “The Action of Carbon Dioxide and of Carbon Monoxide on Manganese”, *Journal of the American Chemical Society*, 1938, vol. 60, No. 12, pp. 3055-3060.